



## Research Paper

Noise-induced cochlear synaptopathy in rhesus monkeys (*Macaca mulatta*)

M.D. Valero <sup>a, b, \*</sup>, J.A. Burton <sup>c</sup>, S.N. Hauser <sup>c</sup>, T.A. Hackett <sup>c</sup>, R. Ramachandran <sup>c, 1</sup>,  
M.C. Liberman <sup>a, b, 1</sup>

<sup>a</sup> Eaton-Peabody Laboratories, Massachusetts Eye and Ear Infirmary, Boston, MA 02114, USA

<sup>b</sup> Department of Otolaryngology, Harvard Medical School, Boston, MA 02115, USA

<sup>c</sup> Vanderbilt University Medical Center, Dept. of Hearing and Speech Sciences, Nashville, TN 37232, USA

## ARTICLE INFO

## Article history:

Received 18 March 2017

Received in revised form

2 June 2017

Accepted 6 July 2017

Available online 8 July 2017

## Keywords:

Noise-induced hearing loss

Cochlear synaptopathy

Non-human primate

Permanent threshold shift

Temporary threshold shift

Cochlear histopathology

## ABSTRACT

Cochlear synaptopathy can result from various insults, including acoustic trauma, aging, ototoxicity, or chronic conductive hearing loss. For example, moderate noise exposure in mice can destroy up to ~50% of synapses between auditory nerve fibers (ANFs) and inner hair cells (IHCs) without affecting outer hair cells (OHCs) or thresholds, because the synaptopathy occurs first in high-threshold ANFs. However, the fiber loss likely impairs temporal processing and hearing-in-noise, a classic complaint of those with sensorineural hearing loss. Non-human primates appear to be less vulnerable to noise-induced hair-cell loss than rodents, but their susceptibility to synaptopathy has not been studied. Because establishing a non-human primate model may be important in the development of diagnostics and therapeutics, we examined cochlear innervation and the damaging effects of acoustic overexposure in young adult rhesus macaques. Anesthetized animals were exposed bilaterally to narrow-band noise centered at 2 kHz at various sound-pressure levels for 4 h. Cochlear function was assayed for up to 8 weeks following exposure via auditory brainstem responses (ABRs) and otoacoustic emissions (OAEs). A moderate loss of synaptic connections (mean of 12–27% in the basal half of the cochlea) followed temporary threshold shifts (TTS), despite minimal hair-cell loss. A dramatic loss of synapses (mean of 50–75% in the basal half of the cochlea) was seen on IHCs surviving noise exposures that produced permanent threshold shifts (PTS) and widespread hair-cell loss. Higher noise levels were required to produce PTS in macaques compared to rodents, suggesting that primates are less vulnerable to hair-cell loss. However, the phenomenon of noise-induced cochlear synaptopathy in primates is similar to that seen in rodents.

© 2017 Elsevier B.V. All rights reserved.

## 1. Introduction

Acoustic overexposure is a significant health concern in the industrialized world. Vulnerable populations include military personnel, professional musicians, miners, and construction workers (McBride, 2004; Humes et al., 2005; Gordon et al., 2016; Schink et al., 2014), but everyday noise-exposure from leisure activities may also threaten cochlear integrity (e.g., Portnuff et al., 2011; Flamme et al., 2012; Le Prell et al., 2012; Liberman et al., 2016). Noise-related damage to the cochlea scales with the

intensity, duration, and number of acoustic overexposures (Harris, 1950; Eldredge et al., 1973; Hawkins et al., 1976; Bohne and Clark, 1982), and the perceptual consequences can range from degradations in temporal processing and speech perception (Plack et al., 2014; Bharadwaj et al., 2014, 2015) to significant impairments in sound detection.

An acoustic overexposure sufficiently intense to damage or destroy outer hair cells (OHCs) and/or their stereocilia will induce permanent threshold shifts (PTS) that are detectable by behavioral audiograms, auditory brainstem responses (ABRs), or distortion-product otoacoustic emissions (DPOAEs) (Wang et al., 2002; Liberman and Dodds, 1984). Exposures that were once thought to be benign, because hair cells were spared and threshold shifts were temporary, are now known to produce primary neuronal degeneration (Kujawa and Liberman, 2009). This degeneration begins immediately as an atrophy of the afferent cochlear synapses

\* Corresponding author. 243 Charles St., Boston, MA 02114, USA.

E-mail address: [michelle\\_valero@meei.harvard.edu](mailto:michelle_valero@meei.harvard.edu) (M.D. Valero).

<sup>1</sup> Ramachandran, R. and Liberman, M.C. are co-senior authors and contributed equally to this work.

between IHCs and auditory nerve fiber (ANFs), and it is followed by a slow retraction of the myelinated distal axons of ANFs that finalizes after months or years with the death of the ANF cell bodies (the spiral ganglion cells) and their central axons projecting to the cochlear nucleus (Johnsson, 1974; Liberman and Kiang, 1978; Felix et al., 2002; Kujawa and Liberman, 2009; Lin et al., 2011). Cochlear synaptopathy may be a key contributor to the differences in speech-in-noise performance among listeners with similar threshold audiograms, a.k.a. hidden hearing loss (Liberman, 2015; Schaette and McAlpine, 2011).

Most of what we know about cochlear synaptopathy is based on studies in mice and guinea pigs (reviewed by Kujawa and Liberman, 2015), but several lines of evidence suggest that humans are less vulnerable to noise damage than smaller mammals (see Dobie and Humes, 2017). Nonetheless, emerging data in humans also suggest that, as in mice and guinea pigs, cochlear neurons are more vulnerable than hair cells. Because the inner ear cannot be biopsied, direct evaluation of cochlear synaptopathy in humans must rely on accrual of post-mortem specimens, and such material is slowly accumulating: normal-aging human ears show minimal hair-cell loss but a progressive primary neural degeneration, i.e. a steady age-related loss of spiral ganglion cells (Makary et al., 2011). Based on a small sample of cases, there appears to be a much more dramatic loss of cochlear synapses in the normal-aging human than can be seen in counts of ganglion cells (Viana et al., 2015), as has been more exhaustively documented in mice (Fernandez et al., 2015). No data are yet available on noise-induced cochlear synaptopathy in humans.

Here, we chose to study noise-induced cochlear synaptopathy in a non-human primate. Given that the physiological processes and biomarkers of human ailments are often closely mirrored in monkeys (e.g., Wendler and Wehling, 2010), these data may be useful in inferring the patterns of human synaptopathy, and a primate model of noise-induced synaptopathy could be key in assessing emerging therapies to reconnect surviving ANFs to IHCs (Wan et al., 2014; Suzuki et al., 2016). We show that rhesus ears are less vulnerable to hair-cell loss and permanent threshold shifts than other well-studied small mammals (cats, guinea pigs, mice, and chinchillas). However, as seen in rodent models (Kujawa and Liberman, 2009; Lin et al., 2011), primate cochlear synapses are more vulnerable than hair cells to acoustic trauma, and many of the IHCs remaining in acoustically traumatized ears are partially or largely deafferented.

## 2. Methods

### 2.1. Animals and groups

Ten rhesus monkeys (*Macaca mulatta*) 6.5–11 yrs of age were included in this study. Seven (5 male, 2 female) were housed at Vanderbilt University, and three (males) at Boston University. At both institutions, animals were on a 12 h light/dark cycle with access to food and water *ad libitum*, except for 12 h prior to physiological testing, noise-overexposure, and euthanasia. Four macaques (3 from Boston University, 1 from Vanderbilt) served as histological controls. The remaining six (from Vanderbilt) were subjected to acoustic overexposure. For all noise-exposed monkeys, cochlear function was measured before and immediately after the exposure, as well as 3–8 times during the 8–9 wks post exposure. All housing and procedural protocols were approved by the respective Institutional Animal Care and Use Committees and were in strict compliance with the guidelines established by the National Institutes of Health.

### 2.2. Acoustic overexposure

Monkeys were treated with atropine (0.04 mg/kg), anesthetized with a mixture of ketamine and dexmedetomidine (2–6 mg/kg and 5–15 µg/kg), intubated, and maintained on 1–1.5% isoflurane for the duration of each 4-hr exposure to a 50-Hz noise band centered at 2 kHz. Noise levels varied for different exposures, and some animals were exposed more than once (Table 1). Noise was presented binaurally via closed-field speakers (MF1 speakers, TDT Inc., Alachua, FL) coupled to the ears with foam inserts. The stability of the transducer output ( $\pm 0.3$  dB) was verified by replacing the monkey with a ¼" microphone (Model 378C01, PCB piezotronics) during a 4-hr exposure session.

### 2.3. Cochlear function tests

Cochlear function tests were conducted in a double-walled sound-attenuating booth at Vanderbilt University (RE-246, Acoustic Systems) under ketamine/dexmedetomidine anesthesia (10–12 mg/kg/hr ketamine, periodic boluses of dexmedetomidine). DPOAEs were measured using a Bio-logic Scout OAE system (Natus) at 8 points per octave from  $f_2 = 0.5$ –8 kHz, with  $f_2/f_1 = 1.22$  and  $L_1/L_2 = 65/55$ . For ABRs, tone bursts were generated and presented at a rate of 27.7 Hz by BioSigRZ software (TDT Inc.), amplified by an SLA2 amplifier (ART Pro Audio, Niagara Falls, NY), and delivered binaurally via SA1 speakers (Selah Audio). At each test frequency, tone-burst level was varied between 30 and 90 dB SPL in 5- or 10-dB steps. Responses were measured via subdermal needle electrodes, vertex-to-mastoid, with the ground at the shoulder. An RA4 pre-amplifier coupled with a RA4LI amplifier (TDT) amplified the signal (10,000X), and the waveform was digitally filtered between 10 Hz and 3 kHz. 1024 artifact-free waveforms were averaged to produce a final ABR trace, and two traces were collected at each stimulus level. Analysis was based on inspection of stacked waveforms. Threshold was defined as the lowest SPL to produce a repeatable waveform  $\geq 120$  nV at the appropriate latency.

### 2.4. Histological preparation

Monkeys from Vanderbilt (all noise-overexposed and one control) were euthanized via an overdose of sodium pentobarbital (130 mg/kg). The three histological control monkeys from B.U. were euthanized by transcardial perfusion with 4 °C Krebs buffer (pH 7.4) followed by 4% paraformaldehyde (pH 7.4), while deeply anesthetized with sodium pentobarbital (25 mg/kg to effect). Following euthanasia, the cochleas were exposed, the round and oval windows were punctured, and cochlear scalae were perfused with the same fixative. Cochleas were submersion-fixed for 2 h and then transferred to 0.12 M EDTA for decalcification. EDTA was refreshed weekly for 3–5 wks, and decalcified tissue was trimmed at each change. Decalcified cochleas were dissected into quarter- or half-turns, and the tissue was cryoprotected in 30% sucrose for 15 min and frozen on dry ice to permeabilize. The pieces were thawed, rinsed in phosphate-buffered saline (PBS; pH 7.3), and incubated in

**Table 1**  
Noise-exposure history for each macaque with TTS and PTS.

Subject ID	108	120	140	146
M1	×	×	×	×
M2	×			×
M3			×	×
M4				×
M5	×			
M6	×			

a blocking reagent (5% NHS with 1% Triton-X in PBS) for 1 h at room temperature. Then, the tissue was transferred to a solution containing primary antibodies (in 1% NHS with 1% Triton-X) to label (1) pre-synaptic ribbons, with mouse (IgG1) anti-CtBP2 (C-terminal binding protein 2; BD Transduction Labs; 1:200); (2) glutamate receptor patches, with mouse (IgG2) anti-GluA2 (Millipore; 1:200) (3) hair cell cytoplasm, with rabbit anti-myosin VIIa (myosin VIIa, Proteus Biosciences; 1:200); and (4) cochlear afferent and efferent fibers, with chicken anti-NFH (neurofilament-H; Chemicon; 1:1000). Following an 18-hr incubation in primary antibodies at 37 °C, the tissue was rinsed in PBS and incubated in species-appropriate secondary antibodies (coupled to AlexaFluor fluorophores) in two separate 1-hr incubations. Finally, the tissue was rinsed and mounted in order (apex to base) in Vectashield (Vector Laboratories, Inc.), and the coverslips were sealed with nail polish. GluA2 immunostaining was unsuccessful in one case (at 1:1000).

### 2.5. Cochlear frequency mapping

Low-magnification images of each cochlea piece were acquired, montaged, and imported into ImageJ. A custom plug-in (freely available at [www.masseyeandear.org/research/otolaryngology/investigators/laboratories/eaton-peabody-laboratories/epl-histology-resources](http://www.masseyeandear.org/research/otolaryngology/investigators/laboratories/eaton-peabody-laboratories/epl-histology-resources)) produced a cochlear frequency map: for each cochlear piece, user-defined points traced along the cuticular plates of IHCs were fit with a spline function, and the total length of the resultant curves was summed. Cochlear frequencies were computed using a Greenwood function (Greenwood, 1990), assuming an upper frequency limit of 45 kHz (Pfungst et al., 1978; Heffner, 2004):  $f(\text{in kHz}) = 360 \times (10^{2.1 \times (1-d)} - 0.85)$ , where  $d$  is the fractional distance from the cochlear base (0–1). Frequency positions between 0.125 and 32 kHz (½-octave intervals) were marked on the montaged images, and frequency maps were used for reference during image acquisition.

### 2.6. Image acquisition

Confocal z-stacks were acquired with a 63× glycerol-immersion objective (N.A. = 1.3) on a Leica TCS SP8 confocal microscope. Cochleas were imaged at places corresponding to each of the test frequencies in the physiological assays. At each place, one stack with x-y raster size of 1024 × 1024 (Fig. 3A'–A'') was acquired at 1X digital zoom to count IHCs and OHCs (Fig. 2). For quantification of IHC synapses, two adjacent stacks were acquired with an x-y raster size of 1024 × 512 and z-steps of 0.33 μm using 2.41X digital zoom. Each stack included the full length (from base to stereocilia tips) of 6–9 IHCs (Fig. 3).

### 2.7. Quantifying synapses and hair cells

Amira software (version 6.0, Visage Imaging) was used to quantify hair cells and afferent synapses in IHC confocal z-stacks. Hair cell survival was assessed in low-power confocal z-stacks (Fig. 2): cuticular plates were counted in the myosin 7a channel and normalized to the expected number of hair cells within each row. To quantify synapses, the “connected components” function algorithmically identified the x-y-z-coordinates and volumes of CtBP2-puncta that 1) exceeded a user-defined intensity threshold and 2) contained at least 10 contiguous pixels. The intensity threshold was set to maximize the inclusion of small ribbons within each stack and minimize ribbon-overlap in the voxel space, and a surface contour of each connected component was displayed along with a maximum projection. Then, any puncta not within hair cells, as determined by myo7a staining, were removed using the “volume edit” function.

To determine whether pre-synaptic ribbons were each paired with an apposing glutamate receptor, a custom C++ program was used to generate an array of high-power thumbnail images from the confocal z-stack using the x-y-z-coordinates in the Amira output. Each thumbnail displayed the x-y projection of a 1-μm voxel cube centered on a ribbon and included any GluA2-positive pixels, representing apposed glutamate receptor patches. “Paired synapses” were those with colocalized red and green puncta (i.e., ribbons with apposed glutamate receptor patches), as determined by visual inspection of the thumbnail arrays, and “orphan ribbons” (solo red puncta; Fig. 3C, white arrows) were excluded from final synapse counts.

### 2.8. Statistics

Statistics were performed in SPSS (IBM, version23). A Kruskal-Wallis test was used to test for significance in threshold shifts, and Wilcoxon-Mann-Whitney rank sum tests, with *post-hoc* Holm-Bonferroni corrections, were used to assess the significance of group differences.

## 3. Results

### 3.1. Cochlear pathophysiology - titrating noise levels to produce TTS vs. PTS

Four monkeys were exposed for 4 h to a narrow-band noise (50 Hz bandwidth, centered at 2 kHz) at 108 dB SPL. Although this exposure would likely produce significant permanent threshold shift (PTS) and hair cell damage in guinea pigs (Lin et al., 2011), chinchillas (Hickox et al., 2016), and cats (Miller et al., 1963, 1997), it caused only a temporary threshold shift (TTS) in these monkeys. The immediate, ~20 dB reduction in DPOAE magnitudes (Fig. 1C, black vs. teal) recovered within 2 wks (not shown), and ABR thresholds and DPOAE magnitudes remained normal 8 wks post-exposure (Fig. 1B, D teal). Two of the four monkeys exposed at 108 dB SPL constituted the ‘TTS group’ for cochlear histopathology. The remaining two were subsequently exposed to higher noise levels.

Four wks following the 108-dB SPL exposure, monkey M1 was re-exposed to the same noise band at 120 dB SPL. Once again, ABR thresholds fully recovered by 1.5 wks post-exposure (not shown). Six wks following this exposure, subject M1 and a naïve monkey (M3) were exposed at 140 dB SPL. Although DPOAE magnitudes did not fully recover to baseline levels by 8 wks post-exposure, only a small mean PTS (~15–18 dB between 2 and 4 kHz) remained at this time point (Fig. 1B, orange). Thus, a final exposure at 146 dB SPL was presented to the three previously exposed monkeys and an additional naïve animal (M4). This exposure produced a severe (30–55 dB) PTS in ABRs between 2 and 16 kHz (Fig. 1B, red), and DPOAEs were immediately and permanently reduced to the noise floor at all frequencies (Fig. 1C and D, red). These 4 monkeys constituted the ‘PTS group’ for cochlear histology. Threshold shifts at 32 kHz are undefined because baseline thresholds ranged from 50 to 75 dB SPL and all post-exposure thresholds at this frequency exceeded the limit of the acoustic system (90 dB SPL). This frequency approaches the upper limits of audibility, where the audiogram steeply slopes in monkeys as young as 5–7 yrs, so high baseline thresholds at 32 kHz may not be pathological (Pfungst et al., 1978; Dylla et al., 2013; Bohlen et al., 2014). Note that ABR threshold shifts in the naïve macaque (M4 in Fig. 1B, Table 1) were similar to those seen in animals with more complicated exposure histories.



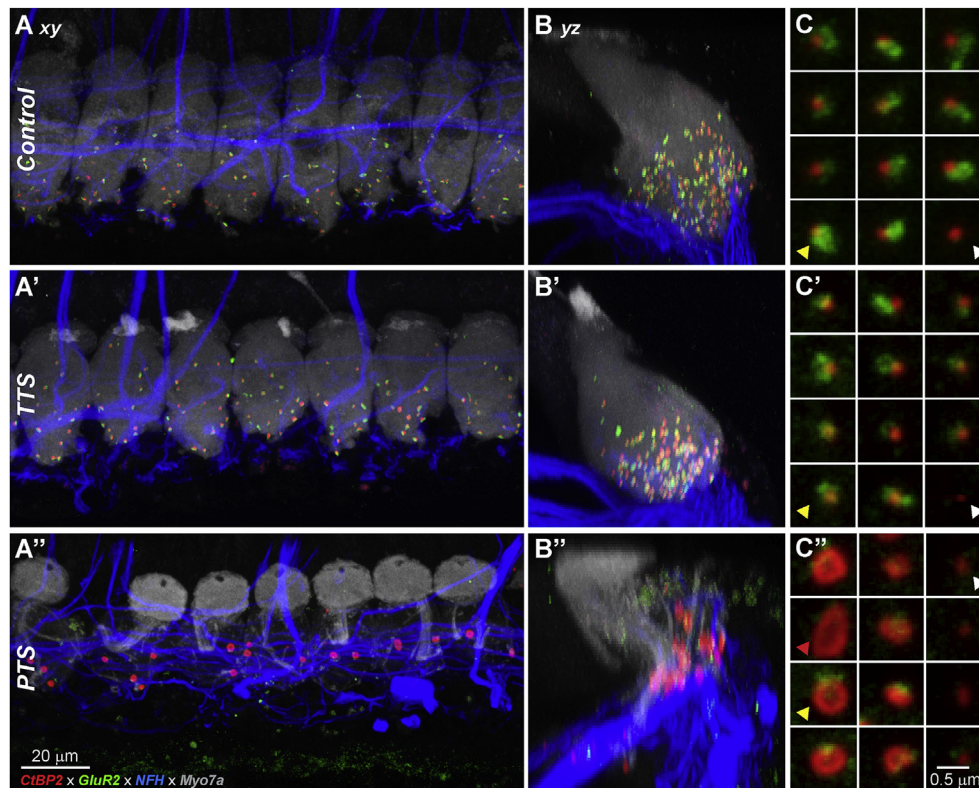


**Fig. 3.** Hair cells and their afferent synapses were visualized by immunohistochemistry. Presynaptic ribbons (CtBP2, red), post-synaptic glutamate-receptor subunits (GluA2, green), hair cells (myo7a; gray), and nerve fibers (NFH, blue) were immunolabeled for confocal microscopy. **A–A'**: Maximum-intensity projections of confocal z-stacks from Control, TTS, and PTS ears at the 4-kHz region and displayed in the acquisition plane. **B–B'**: Orthogonal projections of the z-stacks in A–A'. **C–C'**: Thumbnail array of magnified x-y projections surrounding 12 selected synapses, taken from the z-stacks shown in A–B'. Synapses, i.e. juxtaposed CtBP2 and GluA2 puncta (yellow arrowheads), and “orphan” ribbons, lacking GluA2 puncta (white arrowheads), are shown. Enlarged, hollow ribbons (C'), seen only in severely damaged regions of PTS cochleas, could be either paired or orphaned (yellow and red arrowheads in C', respectively). Images are from an 8 yr-old male control (A–C), an 11 yr-old male with TTS (A'–C'), and a 10 yr-old male with PTS (A''–C'').

### 3.2. Cochlear histopathology

Unexposed controls had nearly full complements of IHCs and OHCs throughout the cochlear spiral (Fig. 2A). In each noise-exposed group, IHCs were less vulnerable than OHCs. The scattered loss of OHCs in TTS cochleas (Fig. 2B) was insufficient to reduce DPOAE magnitudes, at least to moderate-level primary tones (Fig. 1D). Large swaths of hair cells were missing in all PTS cochleas (Fig. 2C): at the 4-kHz frequency place, ~54–100% of OHCs were missing in all except the left ear of monkey M3, in which only ~16% of OHCs were missing. At 8 kHz and above, most PTS ears showed minimal OHC survival (<3% occasionally remaining), except for the left ear of M3, in which most OHCs survived (3% loss). At the 32-kHz frequency place, no hair cells remained in any of the PTS ears. Note that cytochleograms in monkey M4 were similar to the mean traces of the other 3 PTS monkeys (Fig. 2C).

Regions where IHCs, OHCs, and supporting cells were replaced by a thin layer of unspecialized epithelial cells (not shown) were seen in PTS cochleas under light microscopy. These wipe-outs of the organ of Corti were always seen at the basal tip (beyond the 32 kHz place), but wipeouts of varying widths were also observed at mid-cochlear regions (4 kHz region and higher) in many of the cochleas (not shown).

Depending on species and cochlear frequency, IHCs in healthy cochleas are typically innervated by 5–30 ANFs (Liberman et al., 1990). With few exceptions, each ANF terminates in a single synapse on a single IHC (Spendlin, 1969; Liberman, 1980). Thus, counts of ribbons paired with post-synaptic glutamate-receptor

patches (e.g., Fig. 3C) provide an accurate metric of the number of ANFs contacting each IHC. In unexposed controls (Fig. 3A–C, 4A), ANF innervation density was similar to other mammalian species (e.g., mice: Kujawa and Liberman, 2009; humans: Viana et al., 2015; guinea pigs: Furman et al., 2013), i.e., there were, on average, 13–18 synapses/IHC, with lowest densities seen in the apical and basal extremes (Fig. 4A). Synaptic counts were very similar between monkeys housed in separate vivaria (Fig. 4A, thin traces).

Synapse survival after noise (Fig. 4B) was estimated by normalizing synaptic counts in exposed ears to mean control values (Fig. 4A). Monkeys in the TTS group (Fig. 3A'–C') lost, 12–27% of IHC synapses in the basal half of the cochlea, when averaged between 2 and 32 kHz. At the 32 kHz frequency place, individual ears were missing between 13 and 50% of their synapses (mean = 27.1%) (Fig. 4B, teal). Monkeys with PTS suffered more severe synaptopathy; ranging from 59 to 88% (mean = 75%) at the 4-kHz region, one octave basal to the exposure frequency (Fig. 4B, red), even following a single 146-dB SPL exposure (Fig. 4B, case M4). When basal IHCs survived (i.e., at 32 kHz), they were severely de-afferented as well (Fig. 4B, red).

Typically, OHC loss was similar between ears at matched frequency places: the mean interaural difference (across all imaged frequencies) ranged from 4.9 to 16.2% in all but monkey M3, in which the mean interaural difference was 48.1% (Fig. 5). Nevertheless, ABR threshold shifts in M3 were similar between ears in the two ears (not shown) and, like the three other PTS monkeys, DPOAEs in both ears were immediately and permanently immeasurable (with moderate-level primary-tones), suggesting that

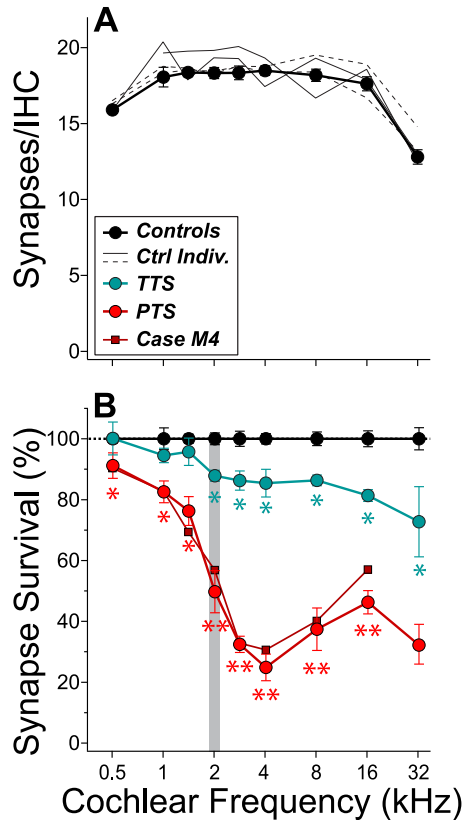


**Fig. 4.** Synapse survival was assessed in IHCs of control (A) and noise-exposed (B) monkeys at nine cochlear regions. A: Mean synaptic counts for  $N = 7$  ears, 4 monkeys are shown by the thick line and filled symbols. Traces for individual monkeys (thin lines) show no differences between animals from the two vivaria. B: Synapse survival is computed by normalizing to the mean data in panel A. TTS (teal) and PTS (red) cochleas had significant, frequency-dependent cochlear synaptopathy. For monkey M4 (single 146-dB SPL exposure), mean synapse survival (L and R) is also plotted separately. Statistical significance is reported relative to controls: \* $P < 0.05$ ; \*\* $P < 0.01$ . Error bars represent  $\pm 1$  SEM. Gray bars represent the exposure band.

stereocilia on surviving basal-turn OHCs were likely damaged (Lieberman and Dodds, 1984). In monkey M3; (Fig. 5A vs. B), the magnitude of synaptopathy in mid-cochlear regions was similar between ears and similar to other PTS cochleas (Fig. 4), despite OHCs being spared in the left ear. This case shows that, in primates, surviving IHCs can lose 60–70% of their afferent synapses in regions with only minimal OHC loss (Fig. 5A), suggesting that, as in mice (Kujawa and Liberman, 2009) and guinea pigs (Lin et al., 2011), the IHC synapses are the first structures in the organ of Corti to degenerate as noise-induced damage increases in severity.

In both mice (Lieberman et al., 2015) and guinea pigs (Furman et al., 2013; Song et al., 2016), surviving ribbons in noise-damaged regions were often larger than normal. Surviving ribbons were also hypertrophied in the noise-exposed macaques (see Fig. 3C, C' vs. C''). Ribbon volumes increased by nearly 350%, on average, in maximally damaged regions of PTS cochleas and by ~175% at the basal extreme of TTS cochleas (Fig. 6A). Many of the abnormally large ribbons in PTS cochleas appeared “hollow” in the CtBP2-labelled micrographs (e.g., Fig. 3C''): two independent observers identified ribbons with dimly labelled cores and brightly labelled outer “shells” (Spearman's  $\rho = 0.987$ ). Quantitative analysis showed that the hollow-ribbon frequency peaked, with a mean of around 35% of imaged ribbons, in the cochlear region just basal to the noise band (Fig. 6B), just as seen for the peak in ribbon hypertrophy (Fig. 6A). Some of these hollow, hypertrophied ribbons were “paired,” or juxtaposed with a post-synaptic glutamate receptor patch (Fig. 3C'', yellow arrow), whereas others were “orphan” ribbons, not in contact with a post-synaptic glutamate receptor patch (Fig. 3C'' red arrow). Prior ultrastructural studies of normal IHCs reported a mixture of ribbons with electron-dense and electron-lucent cores (Lieberman, 1980; Merchan-Perez and Liberman, 1996; Stamatakis et al., 2006), but the “holes” in normal-sized ribbons are presumably below the resolving power of the confocal microscope.

In addition to hair-cell loss and pathological ribbons, there were several other dysmorphologies in noise-exposed IHCs. First, cable-like aggregates of myosin 7a-positive material (Fig. 7A–B) were common in all PTS cochleas, including the animal exposed only once at 146 dB SPL (Fig. 7C, case M4). Their frequency peaked in severely noise-damaged regions (Fig. 7C, red), and they were never seen in control or TTS cochleas. These resembled ‘cytocauds’, the

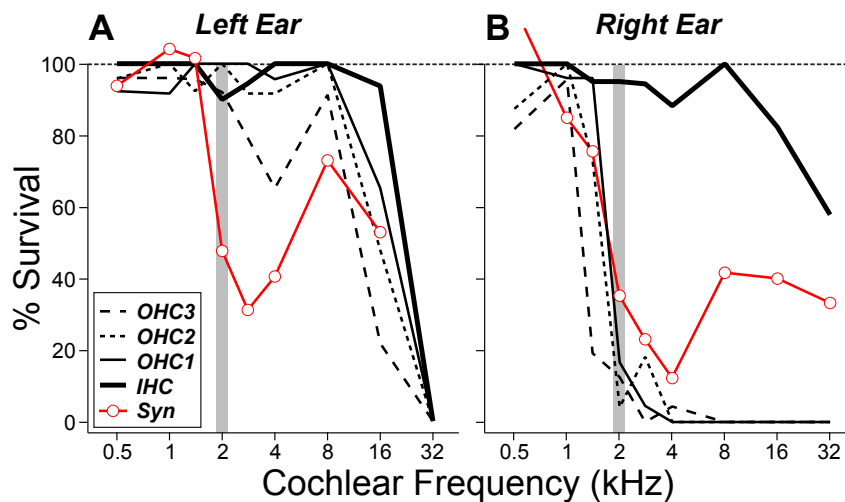


**Fig. 5.** Surviving IHCs were significantly de-afferented in regions with little OHC loss. Cytochromeograms, showing IHC and OHC survival in each row (black), are plotted for left (A) and right (B) ears of a PTS monkey with asymmetric histopathology (M3). The synaptic counts per surviving IHC are overlaid (red). Gray bars represent the exposure frequency. Legend applies to both panels.

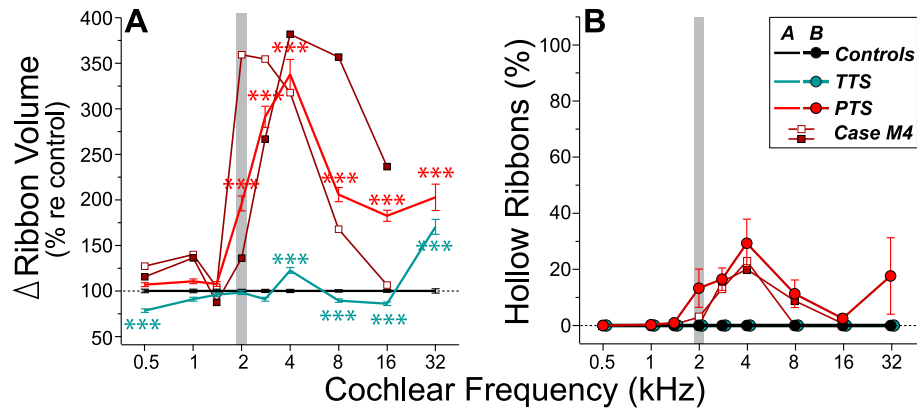


**Fig. 6.** Pre-synaptic ribbons were enlarged in noise-exposed cochleas. Normalized volumes for all pre-synaptic ribbons (A) and the percentage of ribbons classified as “hollow” (B) in controls (black), TTS monkeys (teal), and PTS monkeys (red). Paired and orphan ribbons were included in both analyses. Gray bars represent the exposure band. Error bars represent  $\pm 1$ SEM. For monkey M4 (single 146-dB SPL exposure), the left and right cochleas are plotted separately. Legend applies to both panels. Asterisks represent significance (\*\*\*\* $P < 0.001$ ).

cable-like actin aggregates seen in IHCs and vestibular hair cells from rodents with genetically aberrant stereocilia (Anniko et al., 1980; Sobin et al., 1982; Beyer et al., 2000; Kanzaki et al., 2002; Mathur et al., 2015), suggesting the dysmorphology may be related to noise-induced stereocilia damage. Second, cytoplasmic extrusions were observed in noise-exposed IHCs (Fig. 8A–B). In TTS cochleas, they emanated from the cuticular plate of up to 60% of IHCs in some basal regions (Fig. 8A). Cytoplasmic extrusions at the cuticular plate have been reported as acute, temporary pathologies following noise exposure (e.g., Engström and Borg, 1983), but here they persisted for up to 8 wks post-exposure. In PTS cochleas, cytoplasmic extrusions were seen extending from the base of IHCs into the tunnel of Corti, especially at the 4-kHz region (Fig. 8B).

Third, noise-exposed cochleas had sparsely distributed IHCs with myosin7a-positive nuclei (Fig. 8C, left IHC), a feature never observed in control cochleas. Finally, there was also evidence of missing or fused stereocilia bundles and/or elongated stereocilia on IHCs of both TTS and PTS monkeys (e.g., in Fig. 8C, left IHC, few stereocilia remained).

#### 4. Discussion

A longstanding dogma in noise-exposure studies was that hair cells are most vulnerable to damage, and ANFs degenerate only if they lose their peripheral targets (Bohne and Harding, 2000; Johnsson, 1974). Recent animal studies showed that acoustic

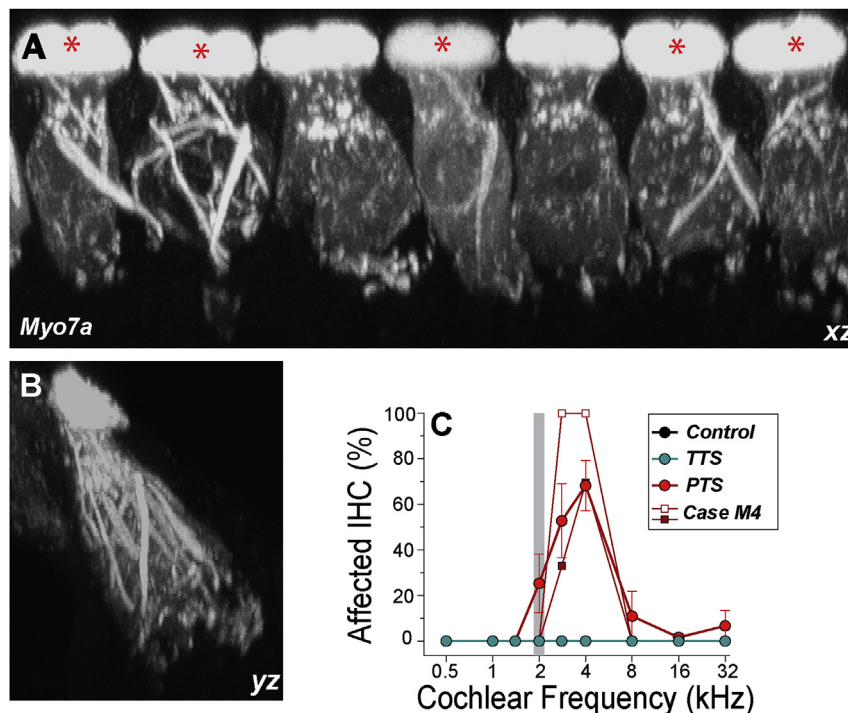


**Fig. 7.** Cable-like myosin aggregates were common in IHCs of PTS ears. Maximum-intensity projections of confocal z-stacks in the x-z plane (A) and y-z plane (B), including 7 IHCs from the 2.8 kHz region in a PTS cochlea. Many IHCs (asterisks in A) show myosin 7a aggregates spanning the apical-basal pole. C: Mean % of affected IHCs for control (black), TTS (teal), and PTS (red) cochleas (N = 7, 4, 8 cochleas, respectively). Error bars represent  $\pm 1$  SEM. Gray bar represents the exposure band.

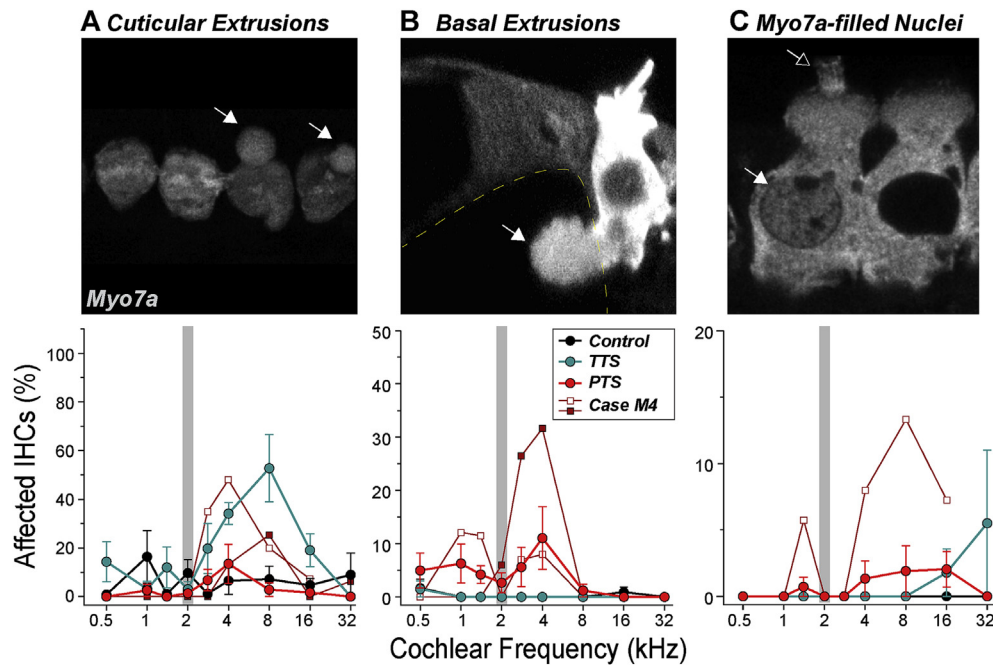


**Fig. 8. IHC pathologies were common in PTS ears.** A–C: Confocal micrographs of pathological IHCs are marked with arrows to indicate: cytoplasmic extrusions from the cuticular plate (A), or the basal pole (B), myosin 7a-positive nuclei (C), and irregular stereocilia (C, open arrow; not quantified). The yellow dashed line in (B) traces the edges of the tunnel of Corti. Plots below each micrograph show the percentage of IHCs affected in each group: For monkey M4 (single 146-dB SPL exposure), data for each ear are plotted separately. Legend in B applies to all panels. Error bars represent  $\pm 1$  SEM. Gray bars represent the exposure band.

overexposures can induce primary neural degeneration, i.e. loss of synapses between ANFs and IHCs, without damaging OHCs or elevating cochlear thresholds (Kujawa and Liberman, 2009; Furman et al., 2013; Hickox et al., 2016). This cochlear synaptopathy went undetected for two reasons: 1) retraction of the peripheral axons of ANFs and the ultimate death of spiral ganglion cells is exceedingly slow (Spoendlin, 1972; Johnsson, 1974), so prior ganglion-cell counts likely overestimated the number of functional ANFs (Viana et al., 2015), and counting synapses under light microscopy required development of antibodies to pre- and post-synaptic proteins; and 2) ANFs with high thresholds and low spontaneous rates (SRs) are most vulnerable to noise damage. Although the loss of this subset is undetected by threshold measures (e.g., Furman et al., 2013; Bourien et al., 2014), the fibers likely contribute to complex listening tasks in noisy environments (Costalupes et al., 1984).

The observation that cochlear synapses and ANF terminals, rather than hair cells, are most vulnerable to noise has now been demonstrated in mice, guinea pigs, chinchillas, rats (reviewed by Hickox et al., 2016), and macaques. Furthermore, cochlear synaptopathy precedes OHC loss and threshold shifts in normally-aging mice (Sergeyenko et al., 2013), it progresses more rapidly if mice were noise-exposed as young adults (Fernandez et al., 2015), and low doses of ototoxic antibiotics can cause cochlear synaptopathy without destroying hair cells or elevating thresholds (Ruan et al., 2014). Thus, in many types of acquired sensorineural hearing loss, there may be significant de-afferentation of surviving IHCs.

The leading hypothesis for the mechanism underlying noise-induced cochlear synaptopathy/neuropathy is that overstimulation of IHCs induces glutamate excitotoxicity in the post-synapse that causes swelling, bursting, and retraction of the terminal dendrite of type-I ANFs (see Liberman and Kujawa, 2017; Ruel et al., 2007 for reviews). This is supported by two observations. First, ANF terminal dendrites swell and retract following application of glutamate

receptor agonists, and this effect is prevented by pre-treatment with glutamate receptor antagonists (Puel et al., 1991, 1994). Similarly, terminal swelling that follows acoustic overexposure is prevented by pre-treatment with glutamate receptor antagonists (Puel and Pujol, 1993). Secondly, following noise trauma, synapses can be regenerated by treatment with exogenous neurotrophins that function in part by promoting axonal outgrowth (e.g., Suzuki et al., 2016).

#### 4.1. Hair cell vulnerability in macaques vs. other mammals

Early primate studies compared behavioral thresholds and cytochleograms in noise-exposed macaques, squirrel monkeys, and others (Stebbins, 1970; Hunter-Duvar and Elliott, 1972; Hawkins et al., 1976; Jerger et al., 1978; Moody et al., 1978; Stebbins et al., 1982), concluding that primates are less susceptible to noise-induced PTS and hair-cell loss than non-primates. In cats and guinea pigs, a PTS of up to ~40–50 dB can be induced by a single 2- or 4-hr exposure to 2-kHz noise between 109 and 113 dB SPL (cats: Liberman and Dodds, 1984; Miller et al., 1997; guinea pigs: Maison and Liberman, 2000; Lin et al., 2011). In contrast, in macaques, a continuous 40-hr exposure to 2-kHz noise at 120 dB SPL produced a peak PTS of only ~20–40 dB (Moody et al., 1978). In squirrel monkeys, inducing a PTS of ~20 dB using a similar traumatic noise required 2–3 exposures totaling 10–14 h (Hunter-Duvar and Elliott, 1972). In humans, a 2-hr exposure at 105 dB SPL caused only a temporary threshold shift (Ward, 1960), as did a 130-dB SPL exposure to a 2 kHz tone for 30 min (Davis et al., 1950). Here, we showed that, in macaques, a 4-hr exposure to a 2-kHz noise at 120 dB SPL caused no PTS, and a 4-hr exposure at 140 dB SPL produced a PTS of <20 dB. Although differences in anesthesia (Kim et al., 2000) and noise bandwidth complicate comparisons, it appears that SPLs must be increased 10-fold (20 dB) to produce a similar degree of moderate PTS in primates vs. non-primates.

When noise-induced PTS is  $\leq 40$  dB, there is typically minimal hair-cell loss, as shown in macaques exposed for 40 h to 2 kHz noise (Moody et al., 1978), because permanent damage to hair-cell stereocilia occurs at lower exposure levels than those producing hair cell death (Robertson, 1982; Liberman and Dodds, 1984). Thus, given that the 140 dB SPL exposure produced PTS  $\leq 20$  dB, it is unlikely that significant hair-cell loss would be observed histologically. As exposure SPL increases, a “critical level” is reached at which hair-cell death grows dramatically. In mice and cats, that critical level is  $\sim 116$  dB SPL for a 2-hr exposure to noise bands centered at mid-cochlear frequency places (Wang et al., 2002; Liberman and Kiang, 1978): at this level, the reticular lamina ruptures during exposure, mixing endolymph and perilymph, resulting in a chronic organ-of-Corti wipeout near the place tuned to the exposure band and widespread OHC loss that spreads basally from that point (Wang et al., 2002). In macaques, the critical level is likely around 146 dB SPL: this exposure caused major OHC loss throughout the basal half of the cochlea and organ-of-Corti wipeouts that appeared usually in mid-cochlear regions, just basal to the exposure frequency, and always in the basal-most ‘hook’ region.

It appears that the primate ear is dramatically less vulnerable to this type of catastrophic noise damage. It is unlikely that this resilience is mediated by the middle-ear muscle reflex (MEMR) or medial olivocochlear reflex (MOCR), based on the observations that central anesthetics attenuate the strength of both reflexes (MEMR: Borg and Moller, 1975; Valero and Liberman, 2017; MOCR: Chambers et al., 2012; Aedo et al., 2015). Such resistance might arise from the mechanical strength of the reticular lamina and the tight junctions that also provide the diffusion barrier between endolymph and perilymphatic scalae. It may be significant that one of the candidate genes in the chromosomal regions linked to differences in noise vulnerability between inbred mouse strains is one of the claudin genes (Street et al., 2014), a major component of the tight junctions in the reticular lamina (Gow et al., 2004).

#### 4.2. Synaptic vulnerability in macaques vs. other mammals

Vulnerability to cochlear synaptopathy also varies between species. In mice synaptopathy can be produced by a single 2-hr exposure to octave-band noise at 94–100 dB SPL (8–16 kHz; Fernandez et al., 2015; Valero and Liberman, 2017), while 106-dB SPL octave-band noise is required to produce synaptopathy in guinea pigs (4–8 kHz; Lin et al., 2011; Furman et al., 2013). Synaptopathy can be seen after exposures producing large TTSs  $\sim 40$ – $50$  dB (24-hrs post-exposure; e.g., Lin et al., 2011; Hickox and Liberman, 2014; Fernandez et al., 2015). However, not all exposures producing large TTSs are synaptopathic (Hickox and Liberman, 2014). Although noise-induced synaptopathy has not been assessed in humans, there is one human study in which TTS was measured 21–23 h (1-d) following exposure to octave-band noise for 2-hrs at 105-dB SPL, and thresholds recovered within 1.5–3 days post-exposure (Ward, 1960). Peak TTS at 1-d post-exposure was  $< 30$  dB in 4/6 subjects and  $\sim 40$  dB in the remaining two. Extrapolating from rodent data, it is possible that this exposure was synaptopathic in the latter two subjects.

Here, we show that a single 4-hr exposure to 108-dB SPL noise produces synaptopathy in primates. These data suggest that although primates may be highly resistant to noise-induced hair-cell destruction, cochlear synapses are not strikingly more resilient than those in other mammals studied to date. The magnitude of synaptopathy in TTS macaques (108-dB SPL exposure) was  $\sim 15$ – $30\%$ , on average (Fig. 4B), which is similar to that observed in guinea pigs at similar SPLs (Liu et al., 2012; Furman et al., 2013; Song et al., 2016). Little is known about the growth of synaptopathy with increasing sound pressure levels, as most studies have

concentrated on exposures producing little or no PTS. Here, we show that synaptopathy can exceed 80% in cochlear regions with significant OHC loss (Figs. 2, 4 and 5).

Each missing or orphaned ribbon is taken to represent a missing synapse, and because each ANF terminates in a single synapse on a single IHC, each missing synapse represents a non-responsive ANF. Due to redundancy in IHC innervation, normal audiometric thresholds can be measured in animals missing as many as 80% of ANFs (Schuknecht and Woellner, 1955) or IHCs (Lobarinas et al., 2013), as long as OHCs remain intact. The subset of ANFs responsible for threshold detection, i.e. fibers with high SRs, are relatively resistant to acoustic trauma, while the low-SR fibers with thresholds normally 30–50 dB higher, are disproportionately disconnected (Furman et al., 2013). Given that low-SR fibers constitute 40–50% of the ANF population (Taberner and Liberman, 1996), and given that thresholds recovered completely following exposure at 108 dB SPL, synaptopathy in TTS macaques should be dominated by loss of low-SR synapses. Macaques with PTS, on the other hand, must be missing both low- and high-SR synapses in maximally damaged regions. Regardless of which SR groups are involved, a loss of up to 88% of ANFs innervating the surviving IHCs is likely to have profound effects on hearing performance in complex listening environments.

Single-fiber labeling of ANFs has shown that low-SR fibers normally terminate opposite large pre-synaptic ribbons, while high-SR fibers terminate opposite smaller ribbons (Merchan-Perez and Liberman, 1996). Thus, ribbons surviving acoustic over-exposure should be smaller if the loss is selective for low-SR fibers and if ribbon volumes are static. However, as seen in mice (Liberman et al., 2015) and guinea pigs (Furman et al., 2013; Song et al., 2016), ribbons were enlarged in the synaptopathic regions of macaque IHCs, especially in PTS cochleas (Fig. 6). Given that ribbon size in zebrafish hair cells is dynamically regulated via negative feedback from synaptic  $\text{Ca}^{2+}$  entry (Sheets et al., 2012), these hypertrophic ribbons may reflect reduced baseline  $\text{Ca}^{2+}$  entry at the synapse. This, in turn, could arise either from changes in the distribution of voltage-gated  $\text{Ca}^{2+}$  channels near the synapse, or from IHC hyperpolarization due to reduced  $\text{K}^{+}$  flux through the stereocilia. Indeed, noise-induced disarray, fusion, or loss of stereocilia in IHC hair bundles (Liberman and Dodds, 1984) should reduce resting currents, hyperpolarize the IHC, and thereby chronically reduce  $\text{Ca}^{2+}$  entry at the synapse. The appearance of hollow ribbons in PTS cochleas may not represent an additional pathology, as both hollow and solid ribbons are seen in electron micrographs of healthy IHCs (Merchan-Perez and Liberman, 1996), and it's likely that hollow ribbon cores could only be resolved in the confocal after noise-induced hypertrophy.

#### Conflict of interest

The authors declare no conflict of interest.

#### Acknowledgements

We are grateful to Drs. Tara Moore and Farzad Mortazavi at Boston University for assistance in tissue acquisition, and we remain ever grateful to Leslie Liberman for expert advice in cochlear immunohistochemistry. Mary Feurtado provided assistance with anesthetic procedures at Vanderbilt. In addition, we thank Dr. Lavinia Sheets for helpful input. Funded in part by NIH R01 DC 00188, NIH P30 DC 005209 (MCL), NIH F32 DC 014405 (MDV), and the Intramural Hobbs Discovery Grant from the Vanderbilt Kennedy Center for Research on Development and Developmental Disabilities (RR). SNH and JAB were partly supported by NIH T35 DC 008763 (L. Hood). Control monkeys from Dr. Tara

Moore's lab at Boston University were funded by NIH R01 AG 043478 (M. Moss) and NIH R01 AG 043640 (D. Rosene).

## References

- Aedo, C., Tapia, E., Elgueda, D., Delano, P.H., Robles, L., 2015. Stronger efferent suppression of cochlear neural potentials by contralateral acoustic stimulation in awake than in anesthetized chinchilla. *Front. Syst. Neurosci.* 9 (21), 1–12. <http://dx.doi.org/10.3389/fnsys.2015.00021>.
- Anniko, M., Sobin, A., Wersall, J., 1980. Vestibular hair cell pathology in the Shaker-2 mouse. *Arch. Otorhinolaryngol.* 226, 45–50.
- Beyer, L.A., Odeh, H., Probst, F.J., Lambert, E.H., Dolan, D.F., Camper, S.A., Kohrman, D.C., Raphael, Y., 2000. Hair cells in the inner ear of the pirouette and shaker 2 mutant mice. *J. Neurocytol.* 29, 227–239.
- Bharadwaj, H.M., Masud, S., Mehraei, G., Verhulst, S., Shinn-Cunningham, B.G., 2015. Individual differences reveal correlates of hidden hearing loss. *J. Neurosci.* 35, 2161–2172.
- Bharadwaj, H.M., Verhulst, S., Shaheen, L., Liberman, M.C., Shinn-Cunningham, B.G., 2014. Cochlear neuropathy and the coding of supra-threshold sound. *Front. Syst. Neurosci.* 8, 26.
- Bohlen, P., Dylla, M., Timms, C., Ramachandran, R., 2014. Detection of modulated tones in modulated noise by non-human primates. *J. Assoc. Res. Otolaryngol.* 15, 801–821.
- Bohne, B.A., Clark, W.W., 1982. Growth of hearing loss and cochlear lesion with increasing duration of noise exposure. In: Hamernik, R.P., Henderson, D., Salvi, R.J. (Eds.), *New Perspectives on Noise-induced Hearing Loss*. Raven, New York, pp. 283–302.
- Bohne, B.A., Harding, G.W., 2000. Degeneration in the cochlea after noise damage: primary versus secondary events. *Am. J. Otol.* 21, 505–509.
- Borg, E., Moller, A.R., 1975. Effect of Central depressants on the acoustic middle ear reflex in rabbit. *Acta Physiol. Scand.* 94, 327–338.
- Bourien, J., Tang, Y., Batrel, C., Huet, A., Lenoir, M., Ladrech, S., Desmadryl, G., Nouvian, R., Puel, J., Wang, J., 2014. Contribution of auditory nerve fibers to compound action potential of the auditory nerve. *J. Neurophysiol.* 112, 1025–1039.
- Chambers, A.R., Hancock, K.E., Maison, S.F., Liberman, M.C., Polley, D.B., 2012. Sound-evoked olivocochlear activation in unanesthetized mice. *J. Assoc. Res. Otolaryngol.* 13, 209–217.
- Costalupes, J.A., Young, E.D., Gibson, D.J., 1984. Effects of continuous noise backgrounds on rate response of auditory nerve fibers in cat. *J. Neurophysiol.* 51, 1326–1344. PMID: 6737033.
- Davis, H., Morgan, C.T., Hawkins Jr., J.E., Galambos, R., Smith, F.W., 1950. Temporary deafness following exposure to loud tones and noise. *Acta-Otolaryngol. Suppl.* 88, 1–56.
- Dobie, R.A., Humes, L.E., 2017. Commentary on the regulatory implications of noise-induced cochlear neuropathy. *Int. J. Audiol.* 56, S74–S78.
- Dylla, M., Hrnicek, A., Rice, C., Ramachandran, R., 2013. Detection of tones and their modification by noise in nonhuman primates. *J. Assoc. Res. Otolaryngol.* 14, 547–560.
- Eldredge, D.H., Miller, J.D., Bohne, B.A., 1973. Anatomical, behavioral, and electrophysiological observation on chinchillas after long exposures to noise. *Adv. Oto. Rhino. Laryngol.* 20, 64–81.
- Engström, B., Borg, E., 1983. Cochlear morphology in relation to loss of behavioural, electro-physiological, and middle ear reflex thresholds after exposure to noise. *Acta Otolaryngol.* S402, 3–23.
- Felix, H., Pollak, A., Gleeson, M., Johnsson, L.G., 2002. Degeneration pattern of human first-order cochlear neurons. *Adv. Otorhinolaryngol.* 59, 116–123.
- Fernandez, K.A., Jeffers, P.W., Lall, K., Liberman, M.C., Kujawa, S.G., 2015. Aging after noise exposure: acceleration of cochlear synaptopathy in “recovered” ears. *J. Neurosci.* 35, 7509–7520.
- Flamme, G.A., Stephenson, M.R., Deiters, K., Tatro, A., van Gessel, D., Geda, K., McGregor, K., 2012. Typical noise exposure in daily life. *Int. J. Audiol.* 51, S3–S11.
- Furman, A.C., Kujawa, S.G., Liberman, M.C., 2013. Noise-induced cochlear neuropathy is selective for fibers with low spontaneous rates. *J. Neurosci.* 110, 577–586.
- Gordon, J.S., Griest, S.E., Thielman, E.J., Carlson, K.F., Helt, W.J., Lewis, M.S., Blankenship, C., Austin, D., Theodoroff, S.M., Henry, J.A., 2016. Audiologic characteristics in a sample of recently-separated military veterans: the noise outcomes in service members epidemiology study (NOISE study). *Hear. Res.* 1–10. <http://dx.doi.org/10.1016/j.heares.2016.11.014>.
- Gow, A., Davies, C., Southwood, C.M., Frolenkov, G., Chrustowski, M., Ng, L., Yamauchi, D., Marcus, D.C., Kachar, B., 2004. Deafness in Claudin 11-null mice reveals the critical contribution of basal cell tight junctions to stria vascularis function. *J. Neurosci.* 24, 7051–7062.
- Greenwood, D.D., 1990. A cochlear frequency-position function for several species - 29 years later. *J. Acoust. Soc. Am.* 87, 2592–2605.
- Harris, J.D., 1950. On latent damage to the ear. *J. Acoust. Soc. Am.* 27, 177–179.
- Hawkins Jr., J.E., Johnsson, L.G., Stebbins, W.C., Moody, D.B., Coombs, S.L., 1976. Hearing loss and cochlear pathology in monkeys after noise exposure. *Acta otolaryngol* 81, 337–343.
- Heffner, R.S., 2004. Primate hearing from a mammalian perspective. *Anat. Rec. Part A* 281A, 1111–1122.
- Hickox, A.E., Liberman, M.C., 2014. Is noise-induced cochlear neuropathy key to the generation of hyperacusis or tinnitus? *J. Neurophysiol.* 111, 552–564.
- Hickox, A.E., Larsen, E., Heinz, M.G., Shinobu, L., Whitton, J.P., 2016. Translational issues in cochlear synaptopathy. *Hear. Res.* <http://dx.doi.org/10.1016/j.heares.2016.12.010>.
- Humes, L., Joellenbeck, L., Durch, J., 2005. Noise and Military Service: Implications for Hearing Loss and Tinnitus. National Academies, Washington, DC.
- Hunter-Duvar, I.M., Elliott, D.N., 1972. Effects of intense auditory stimulation: hearing losses and inner ear changes in the squirrel monkey. *J. Acoust. Soc. Am.* 52, 1181–1192.
- Jerger, J., Mauldin, L., Igarashi, M., 1978. Impedance audiometry in the squirrel monkey. Sensorineural losses. *Arch. Otolaryngol.* 104, 559–563.
- Johnsson, L.G., 1974. Sequence of degeneration of Corti's organ and its first-order neurons. *Ann. Otol. Rhinol. Laryngol.* 83, 294–303.
- Kanzaki, S., Beyer, L.A., Canlon, B., Melchner, W.M., Raphael, Y., 2002. The cytoskeleton: a hair cell pathology in the Waltzing Guinea pig. *Audiol. Neuro-Otol.* 7, 289–297.
- Kim, J.U., Lee, H.J., Kang, H.H., Shin, J.W., Ku, S.W., Ahn, J.H., Kim, Y.J., Chung, J.W., 2000. Protective effect of isoflurane anesthesia on noise-induced hearing loss in mice. *Laryngoscope* 115, 1996–1999.
- Kujawa, S.G., Liberman, M.C., 2009. Adding insult to injury: cochlear nerve degeneration after “temporary” noise-induced hearing loss. *J. Neurosci.* 29, 14077–14085.
- Kujawa, S.G., Liberman, M.C., 2015. Synaptopathy in the noise-exposed and aging cochlea: primary neural degeneration in acquired sensorineural hearing loss. *Hear. Res.* 330, 191–199.
- Le Prell, C.G., Dell, S., Hensley, B., Hall III, J.W., Campbell, K.C.M., Antonelli, P.J., Green, G.E., Miller, J.M., Guire, K., 2012. Digital music exposure reliably induces temporary threshold shift (TTS) in normal hearing human subjects. *Ear Hear* 33, 44–58.
- Liberman, M.C., 1980. Morphological differences among radial afferent fibers in the cat cochlea: an electron-microscopic study of serial sections. *Hear. Res.* 3, 45–63.
- Liberman, M.C., 2015. Hidden hearing loss. *Sci. Am.* 313, 48–53. PMID: 26349143.
- Liberman, M.C., Dodds, L.W., 1984. Single-neuron labeling and chronic cochlear pathology. III. Stereocilia damage and alterations of threshold tuning curves. *Hear. Res.* 16, 55–74.
- Liberman, M.C., Dodds, L.W., Pierce, S., 1990. Afferent and efferent innervation of the cat cochlea: quantitative analysis with light and electron microscopy. *J. Comp. Neurol.* 301, 443–460.
- Liberman, M.C., Kiang, N.Y.S., 1978. Acoustic trauma in cats, cochlear pathology and auditory-nerve activity. *Acta Otolaryngol. Suppl.* 358, 1–63.
- Liberman, M.C., Kujawa, S.G., 2017. Cochlear synaptopathy in acquired sensorineural hearing loss: manifestations and mechanisms. *Hear. Res.* 349, 138–147.
- Liberman, M.C., Epstein, M.J., Cleveland, S.S., Wang, H., Maison, S.F., 2016. Toward a differential diagnosis of hidden hearing loss in humans. *PLoS One* 11 (9), e0162726. <http://dx.doi.org/10.1371/journal.pone.0162726>.
- Liberman, M.C., Suzuki, J., Liberman, L.D., 2015. Dynamics of cochlear synaptopathy after acoustic overexposure. *J. Assoc. Res. Otolaryngol.* 16, 205–219.
- Lin, H.W., Furman, A.C., Kujawa, S.G., Liberman, M.C., 2011. Primary neural degeneration in the Guinea pig cochlea after reversible noise-induced threshold shift. *J. Assoc. Res. Otolaryngol.* 12, 605–616.
- Liu, L., Wang, H., Shi, L., Almukass, A., He, T., Aiken, S., Bance, M., Yin, S., Wang, J., 2012. Silent damage of noise on cochlear afferent innervation in Guinea pigs and the impact on temporal processing. *PLoS One* 7, 1–11.
- Lobarinas, E., Salvi, R., Ding, D., 2013. Insensitivity of the audiogram to carboplatin induced inner hair cell loss in chinchillas. *Hear. Res.* 302, 113–120.
- Maison, S.F., Liberman, M.C., 2000. Predicting vulnerability to acoustic injury with a non-invasive assay of olivocochlear reflex strength. *J. Neurosci.* 20, 4701–4707.
- Makary, C.A., Shin, J., Kujawa, S.G., Liberman, M.C., Merchant, S.N., 2011. Age-related primary cochlear neuronal degeneration in human temporal bones. *J. Assoc. Res. Otolaryngol.* 12, 711–717.
- Mathur, P.D., Vijayakumar, S., Vashist, D., Jones, S.M., Jones, T.A., Yang, J., 2015. A study of whirlin isoforms in the mouse vestibular system suggests potential vestibular dysfunction in DFNB31-deficient patients. *Hum. Mol. Gen.* 24, 7017–7030.
- McBride, D.I., 2004. Noise-induced hearing loss and hearing conservation in mining. *Occ. Med.* 54, 200–206.
- Merchan-Perez, A., Liberman, M.C., 1996. Ultrastructural differences among afferent synapses on cochlear hair cells: correlations with spontaneous discharge rate. *J. Comp. Neurol.* 371, 208–221.
- Miller, J.D., Watson, C.S., Covell, W.P., 1963. Deafening effects of noise on the cat. *Acta Otolaryngol. Suppl.* 176, 1–81.
- Miller, et al., 1997. Effects of acoustic trauma on the representation of the vowel/e/in cat auditory nerve fibers. *J. Acoust. Soc. Am.* 101, 3602–3616.
- Moody, D.B., Stebbins, W.C., Hawkins, J.E., Johnsson, L.G., 1978. Hearing loss and cochlear pathology in the monkey. *Arch. Otorhinolaryngol.* 220, 47–72.
- Pfingst, B.E., Laycock, J., Flammino, F., Lonsbury-Martin, B., Martin, G., 1978. Pure tone thresholds for the rhesus monkey. *Hear. Res.* 43–47.
- Plack, C.J., Barker, D., Prendergast, G., 2014. Perceptual consequences of “hidden” hearing loss. *Trends Hear.* 18, 1–11.
- Portnuff, C.D., Fligor, B.J., Arehart, K.H., 2011. Teenage use of portable listening devices: a hazard to hearing? *J. Am. Acad. Audiol.* 22, 663–677.
- Puel, J.-L., Pujol, R., 1993. Recent advances in cochlear neurobiology: cochlear efferents and acoustic trauma. In: Vallet, M. (Ed.), *Noise and Man*. INRETS, pp. 136–145. Actes no 34 ter.
- Puel, J.-L., Pujol, R., Ladrech, S., Eybalin, M., 1991.  $\alpha$ -Amino-3-hydroxy-5-methyl-4-

- isoxazole propionic acid (AMPA) electrophysiological and neurotoxic effects in the Guinea pig cochlea. *Neuroscience* 45, 63–72.
- Puel, J.-L., Pujol, R., Tribillac, F., Ladrech, S., Eybalin, M., 1994. Excitatory amino acid antagonists protect cochlear auditory neurons from excitotoxicity. *J. Comp. Neurol.* 341, 241–256.
- Robertson, D., 1982. Effects of acoustic trauma on stereocilia structure and spiral ganglion cell tuning properties in the Guinea pig cochlea. *Hear. Res.* 7, 55–74.
- Ruan, Q., Ao, H., He, J., Chen, Z., Yu, Z., Zhang, R., Wang, J., Yin, S., 2014. Topographic and quantitative evaluation of gentamicin-induced damage to peripheral innervation of mouse cochlea. *Neurotoxicol* 40, 86–96.
- Ruel, J., Wang, J., Rebillard, G., Eybalin, M., Lloyd, R., Pujol, R., Puel, J.L., 2007. Physiology, pharmacology and plasticity at the inner hair cell synaptic complex. *Hear Res.* 227, 19–27.
- Schaette, R., McAlpine, D., 2011. Tinnitus with a normal audiogram: physiological evidence for hidden hearing loss and computational model. *J. Neurosci.* 31, 13452–13457.
- Schink, T., Kreutz, G., Busch, V., Pigeot, I., Ahrens, W., 2014. Incidence and relative risk of hearing disorders in professional musicians. *Occup. Environ. Med.* 71, 472–476.
- Schuknecht, H.F., Woellner, R.C., 1955. An experimental and clinical study of deafness from lesions of the cochlear nerve. *J. Laryngol. Otol.* 69, 75–97.
- Sergeyenko, Y., Lall, K., Liberman, M.C., Kujawa, S.G., 2013. Age-related cochlear synaptopathy: an early-onset contributor to auditory functional decline. *J. Neurosci.* 33, 13686–13694.
- Sheets, L., Kindt, K.S., Nicolson, T., 2012. Presynaptic Cav1.3 channels regulate synaptic ribbon size and are required for synaptic maintenance in sensory hair cells. *J. Neurosci.* 32, 17273–17286.
- Sobin, A., Anniko, M., Flock, A., 1982. Rods of actin filaments in type I hair cells of the Shaker-2 mouse. *Arch. Otorhinolaryngol.* 236, 1–6.
- Song, Q., Shen, P., Li, X., Liu, L., Wang, J., Yu, Z., Stephen, J., Aiken, S., Yin, S., Wang, J., 2016. Coding deficits in hidden hearing loss induced by noise: the nature and impacts. *Sci. Rep.* 6, e25200. <http://dx.doi.org/10.1038/srep25200>.
- Spoendlin, H., 1969. Innervation patterns in the organ of Corti of the cat. *Acta Otolaryngol.* 67, 239–254.
- Spoendlin, H., 1972. Innervation densities of the cochlea. *Acta Otolaryngol.* 73, 235–248.
- Stamatakis, S., Francis, H.W., Lehar, M., May, B.J., Ryugo, D.K., 2006. Synaptic alterations at inner hair cells precede spiral ganglion cell loss in aging C57BL/6J mice. *Hear. Res.* 221, 104–118.
- Stebbins, W.C. (Ed.), 1970. *Studies of Hearing and Hearing Loss in the Monkey*. Appleton-Century-Crofts, New York.
- Stebbins, W.C., Moody, D.B., Serafin, J.V., 1982. Some principal issues in the analysis of noise effects on hearing in experimental animals. *Am. J. Otolaryngol.* 3, 295–304.
- Street, V.A., Kujawa, S.G., Manichaikul, A., Broman, K.W., Kallman, J.C., Shilling, D.J., Iwata, A.J., Robinson, L.C., Robbins, C.A., Li, J., Liberman, M.C., Tempel, B.L., 2014. Resistance to noise-induced hearing loss in 129S6 and MOLF mice: identification of independent, overlapping, and interacting chromosomal regions. *J. Assoc. Res. Otolaryngol.* 15, 721–738.
- Suzuki, J., Corfas, G., Liberman, M.C., 2016. Round-window delivery of neurotrophin-3 regenerates cochlear synapses after acoustic overexposure. *Sci. Rep.* 6, 24907. <http://dx.doi.org/10.1038/srep24907>.
- Taberner, A.M., Liberman, M.C., 1996. Response properties of single auditory nerve fibers in the mouse. *J. Neurophysiol.* 93, 557–569. PMID: 15456804.
- Valero, M.D., Liberman, M.C., 2017. Effects of Cochlear Synaptopathy on the Middle-ear Muscle Reflex in Unanesthetized Mice. *Association for Research in Otolaryngology*, Baltimore, MD.
- Viana, L.M., O'Malley, J.T., Burgess, B.J., Jones, D.D., Oliviera, C.A.C.P., Santos, F., Merchant, S.N., Liberman, L.D., Liberman, M.C., 2015. Cochlear neuropathy in human presbycusis: confocal analysis of hidden hearing loss in post-mortem tissue. *Hear. Res.* 327, 78–88.
- Wan, G., Gomez-Casati, M.E., Gigliello, A.R., Liberman, M.C., Corfas, G., 2014. Neurotrophin-3 regulates ribbon synapse density in the cochlea and induces synapse regeneration after acoustic trauma. *eLife* 3.
- Wang, Y., Hirose, K., Liberman, M.C., 2002. Dynamics of noise-induced cellular injury and repair in the mouse cochlea. *J. Assoc. Res. Otolaryngol.* 3, 248–268.
- Ward, W.D., 1960. Recovery from high values of temporary threshold shift. *J. Acoust. Soc. Am.* 32, 497–500.
- Wendler, A., Wehling, M., 2010. The translatability of animal models for clinical development: biomarkers and disease models. *Curr. Opin. Pharmacol.* 10, 601–606.